https://doi.org/10.5194/egusphere-2025-538
Preprint. Discussion started: 25 February 2025

Tectonic controls on the formation and evolution of internally drained systems in the western Betics fold-and-thrust belt (S Spain)

Alejandro Jiménez-Bonilla (1), Manuel Díaz-Azpiroz (1), Miguel Rodríguez-Rodríguez (1), Juan Carlos Balanyá (1), Jose Luis Yanes (1), Inmaculada Expósito (1)

(1) Physical, Chemical and Natural Department, University Pablo de Olavide, Seville, Spain

Corresponding author: Alejandro Jiménez Bonilla ajimbon@upo.es

Abstract

We analyse the drainage network in a depressed area within the western Betics fold-and-thrust belt (southern Spain) to investigate the Atlantic-Mediterranean water divide evolution after the Messinian Salinity Crisis (last 5 My). To do that, we made a hydro -geomorphic evaluation of streams and endorheic basins together with a detailed field-based analyses of post-Serravallian structural features. Results from the analysis of stream profiles and the application of SLk and χ indexes showed that Mediterranean streams present a higher incision capacity than Atlantic streams, tributaries of the Guadalquivir river. Moreover, several rivers captures of Atlantic river watersheds and of endorheic basins have been described and quantified. Although the Atlantic-Mediterranean water divide will probably move NW-ward, endorheic basins will still endure, hosted in a depressed area located between two active transpressive zones (the Algonales-Badolatosa and Torcal shear zones). Our results confirm that active tectonics have reshaped the area more intensively than previously considered, and that this modification had significant hydrological implications.

https://doi.org/10.5194/egusphere-2025-538
Preprint. Discussion started: 25 February 2025

Keywords: Surface uplift, shear zones, playa-lake, χ index, water divide.

1. Introduction

The topography of active mountain belts results from the competing interplay between internal and external geodynamic controls. Thus, mantle convection, tectonics and isostasy interact with climate and surface processes to shape the evolving landscape of these regions (e.g., Bahadori et al., 2022, and references therein).

In this regard drainage networks are particularly sensitive to transient topographic signals, undergoing changes in stream long-profiles and flow-directions, as well as topological reshape of basins by means of stream captures or basin divisions.(e.g. Babault et al., 2012; Giletycz et al., 2015; Winterberg and Willett, 2019). Afterward, drainage networks equilibrium is achieved in relatively short time, from 1000 to 100,000 yr., although the lithology, the climate or the watershed size may change this timespan (Whipple and Tucker, 1999; Korup, 2006).

It is for this reason that both qualitative and quantitative analysis of drainage systems have often been used for the characterization of active tectonics (e.g. Pérez-Peña et al., 2010; Azañón et al., 2015). Nevertheless, endorheic basins have been rarely analysed for such purpose, despite the fact that tectonics often governs topographic barriers that enclose such basins, both favouring their inception and conditioning their subsequent evolution. These internally drained systems are identified in a great variety of tectonic scenarios such as rift systems (Río Grande and East African Rifts; Repasch et al., 2017; Berry et al., 2019), foreland basins (Duero basin; Anton et al., 2014), intramontane basins

https://doi.org/10.5194/egusphere-2025-538
Preprint. Discussion started: 25 February 2025

(Giano and Schiattarella, 2023) and contractional belts (Puna-Altiplano and Tibetian Plateau; Sobel et al., 2003). These endorheic basins usually host wetlands, playa-lakes and ponds that depend on their water balances to be ecologically functional. The ratio between the average flooded surface (AFS) and its watershed surface (W) is relevant in the endowment of the hydrological functioning of such ecosystems (Rodríguez-Rodríguez et al., 2012). Active tectonics may modify the watershed area, and, as a consequence, the absolute water input, which results in AFS variations (Jiménez-Bonilla et al., 2023).

In the case of the Betic chain of southern Spain, endorheic areas cover much of both the internal zones (Mather, 2000; Stokes et al. 2019), and the fold-and-thrust belt, as well as its transition to the foreland basin, since the Pliocene (Medina, 1991; Rodríguez-Rodríguez et al., 2009; 2012; Jiménez-Bonilla et al., 2023). Our case study focuses on a depressed area related to the current Atlantic-Mediterranean divide within the western Betics fold-and-thrust belt (Figs. 1 and 2). This area is characterized by a particularly dense cluster of playa-lakes and ponds (e.g. Rodríguez-Rodríguez, 2007; Rodríguez-Rodríguez et al., 2016). Because of their location near the headwater of highly energetic Mediterranean rivers, their existence is often ephemeral (ca. 1000 yrs.; Rodríguez-Rodríguez et al., 2016).

Before the Atlantic-Mediterranean water divide inception, this area included one of the upper Miocene Atlantic-Mediterranean corridors: the Guadalhorce gateway (Martín et al., 2001; 2014). During this age, shallow marine sediments deposited in this area, which are currently uplifted more than 100 m. a.s.l. The Guadalhorce gateway closure, which is not yet fully understood, contributed to the isolation of the Mediterranean Sea and the subsequent Messinian Salinity Crisis (MSC), responsible for the significant drop of the Mediterranean Sea level. Previous works have proposed that the huge erosion volume associated with this event was compensated by an isostatic rebound of the

https://doi.org/10.5194/egusphere-2025-538
Preprint. Discussion started: 25 February 2025

Mediterranean watershed, thus uplifting the topographic relief associated with the post-Tortonian Atlantic-Mediterranean divide (Elez et al., 2016; 2020). Nevertheless, this assumption is not supported by the characterization of structures potentially compatible with this mechanism. Interestingly, the current Atlantic-Mediterranean divide, coincides with the NW-ward migrating front of the Betic fold-and-thrust belt, dominated in our study area by right-lateral transpression (Díaz-Azpiroz et al., 2014; Barcos et al., 2015; Jiménez-Bonilla et al., 2015). In this regard, it is worth noting that recent works have suggested that the permanence of the above mentioned playa-lakes seems to depend on the ongoing tectonic activity in the area (Rodríguez-Rodríguez et al., 2009; Jiménez-Bonilla et al., 2023).

Thus. our first, broad objective is to explore the nature of the main factors that control the evolution of the Atlantic-Mediterranean divide, as well as the inception and later development of the endorheic systems from the MSC to the Holocene. To do that, we zoom into this time frame to analyse in detail the evolution of the late Quaternary playa-lake systems: timing, reshaping and fluvial captures. We explore the drainage network of both exorheic and endorheic watersheds combining the characterization of streams (stream profile, stream length-gradient index and χ index) with the analysis of the change in both shape and distribution of endorheic systems. We combine these geomorphic tools with the kinematic analysis of the recent to active tectonic structures, and we estimated the differential post-Tortonian uplift.

2. Main geological and geomorphological features of the study area

The Neogene collision between the Alboran domain and the Iberian and Maghrebian paleomargins built up the Gibraltar arc, which is composed of two branches: the Betics to the N and the Rif to the S (e.g., Vera, 2004; Fig. 1A). Between both paleomargins and the Alboran domain, Flysch Trough units were deposited. Both paleomargin-derived and Flysch units were

https://doi.org/10.5194/egusphere-2025-538
Preprint. Discussion started: 25 February 2025

deformed into the Betics and Rif fold-and-thrust belts. At the concave side of the arc, a marine back-arc basin developed (Comas et al., 1999; Fig. 1A).

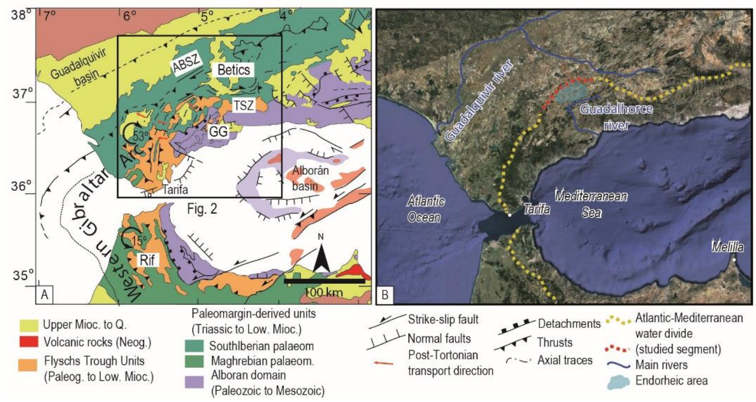

Fig. 1. (A) Tectonic map that shows the main structures (GG: Guadalhorce gateway) and (B) ortorphoto that includes the Atlantic-Mediterranean water divide and main rivers of the Betics chain (TSZ: Torcal Shear Zone; ABSZ: Algodonales-Badolatosa Shear Zone) © Google Earth image from 2021.

The Betics fold-and-thrust belt records two main deformation events: a lower to middle Miocene main deformation related to the external orogenic wedge accretion (Balanyá et al., 2007; Expósito et al., 2012) and a post-Serravallian deformation responsible for the current major relief features (Barcos et al., 2015; Jiménez-Bonilla et al., 2015; 2017). The post-Tortonian uplift is heterogeneous along and across the Betics, reaching the highest values (ca. 1,600 m) in the Eastern Betics, and more than 700 m in the Western Betics (Sanz de Galdeano and Alfaro, 2004; Jiménez-Bonilla et al., 2015; 2017).

During this post-Serravallian event, the second-order, the western Gibraltar arc became individualized as the westernmost salient of the Gibraltar arc (west of 4º30, Fig. 1). The individualization of the western Gibraltar arc has been accommodated in the northern branch, i.e., the Betics, by two dextral, transpressional shear zones (Jiménez-Bonilla et al., 2015; Díaz-Azpiroz et al., 2014; Barcos et al., 2015): the Torcal Shear Zone and the Algodonales-Badolatosa Shear Zone (TSZ and ABSZ, respectively; Fig. 2). This kinematics sharply contrast with that observed in the frontal part of the western Gibraltar arc, characterized by arc–parallel shortening structures and arc-perpendicular stretching structures (Balanyá et al., 2007; 2012; Jiménez-Bonilla et al., 2015; 2017; Figs. 1 and 2).

The post-Serravalian structures provoke a significant structural and topographic relief compartmentation where mountain ranges are interrupted by depressions along and across the fold-and-thrust belt (Fig. 2). Our study is focused on a roughly triangular depressed area, hereafter called as the Antequera Depressed Area (ADA), limited by the two above-mentioned post-Serravallian, dextral transpressive zones (Fig.2), located close to the contact with the Alboran domain.

The ADA shows a low-lying relief at about 400 m.a.s.l. and it is characterized by the development of endorheic basins since the Pliocene (Medina, 1991; Höbig et al., 2016). It is surrounded by areas rising over 100 m above this topographical depression, being the sharpest relief drops found in its NW, SE and SW boundaries (Fig. 2).

The ABSZ spatially coincides with the NW limit of the ADA. It is 90 km long and builds up SW-NE oriented mountain ranges that can be higher than 800 m (Fig. 2). It can be divided into three main segments, which are connected by NW-SE relay zones (Jiménez-Bonilla et al., 2015; Díaz-Azpiroz et al., 2020). To the SE of the ADA, the TSZ constitutes a 70 km long topographic high (up to 1,500 m), oriented approximately W-E (Fig. 2). The TSZ western segment (wTSZ in Figs. 2 and 3), has been interpreted as the tip zone of the TSZ. It consists of two WNW-ESE dextral strike-slip fault zones connected by a compressive bridge (Jiménez-Bonilla et al., 2013; Barcos et al., 2015).

The rocks involved in our study area are mainly derived from the South-Iberian paleomargin. They belong to the Subbetic units (Vera et al., 2004), which are composed of: (1)

https://doi.org/10.5194/egusphere-2025-538
Preprint. Discussion started: 25 February 2025

Triassic clays, gypsum and marls, with isolated hm-scale dolostone bodies, (2) Jurassic dolostones and limestones and (3) Cretaceous to Paleogene marls and marly-limestones that generally form isolated outcrops. Recent works have pointed out that the scarce hills that interrupt the ADA flat topography are controlled by pop-up structures that uplift Jurassic limestones underlain by a major allochthonous Triassic canopy (Flinch and Soto, 2017; 2022; Fig. 2B). Upper Miocene sediments unconformably lie over the Subbetic units (Martín et al., 2001; Fig. 2B). Tortonian sedimentary rocks in the study area consists of calcirudites and calcarenites with shallow water fossils (pectinidae, ostreidae, sea urchins) and syn-sedimentary structures pointing to a moderate to high energetic deposition medium (cross bedding). Therefore, these formations may be a good proxy to the upper-Miocene sea level (Sanz de Galdeano and Alfaro, 2004). Continental sediments were deposited unconformably during the Pliocene to Quaternary. Pliocene sediments include clasts from the Alborán domain, located to the S. Quaternary deposits mainly correspond to alluvial terraces, associated with the main rivers, alluvial fans and pediments. Lacustrine dark quaternary sediments are well represented, being often useful to identify paleo playa lakes. Some of these outcrops are larger than 1,000 hm^2.

The Quaternary Atlantic-Mediterranean water divide runs parallel to the Betics main trend. In the ADA, it is highly diffuse because of the presence, near the divide, of several endorheic systems (Fig. 2). The watersheds of these systems are located within the Atlantic or the Mediterranean watersheds. The Mediterranean and Atlantic watersheds are drained by Guadalhorce and Guadalquivir tributaries, respectively (Fig. 2).

https://doi.org/10.5194/egusphere-2025-538
Preprint. Discussion started: 25 February 2025

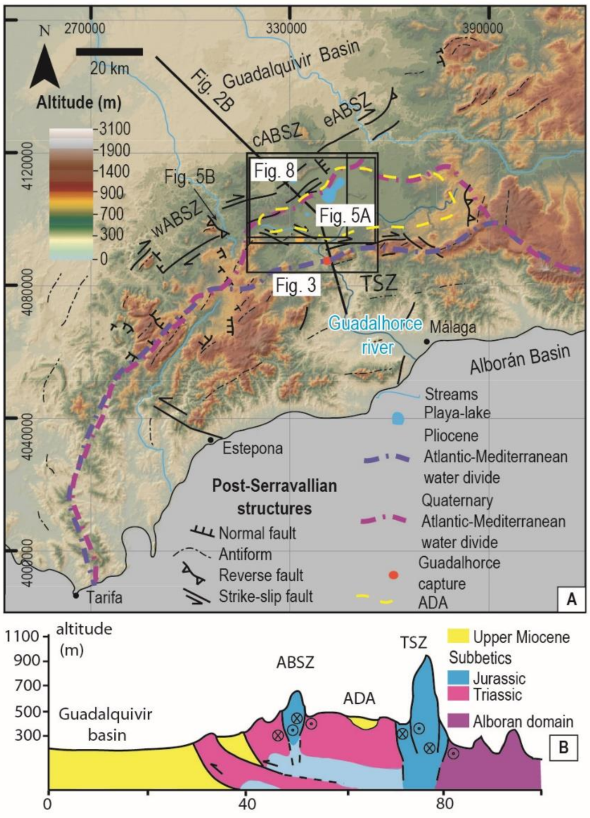

Fig. 2. (A) Relief map of the western Betics showing the main post-Serravallian structures and the Atlantic-Mediterranean water divide in the Pliocene and in the Quaternary (Junta de Andalucía, 2016). (B) Geological cross-section across the western Betics that shows the main structures of the Betics fold-and-thrust belt. TSZ: Torcal Shear Zone; ABSZ: Algodonales-Badolatosa Shear Zone; ADA: Antequera Depressed Area. See location in Fig. 1A.

3. Methodology

This work is an interdisciplinary study that combines structural and geomorphologic analyses, also including hydrogeological data and analytical modelling related to uplift.

3.1. Uplift estimates

One of the main topics of this work is estimating the differential surface uplift from the Tortonian onwards and its possible linkage with upper Miocene deformation at specific shear zones. The former is obtained from a map that includes the current altitude of all marine, shallow water, upper-Miocene sediments in the study area (Fig. 3). The possible contribution of upper Miocene transpression at the TSZ to this differential uplift is evaluated by kinematic modelling. From a mathematical point of view, transpression is a combination of simple shearing parallel to the shear zone and a coaxial component that produces shortening across the shear zone and extrusion parallel to it (e.g., Sanderson and Marchini, 1984). Fernández et al. (2013) expanded the model of Schulmann et al. (2003) to calculate the vertical uplift *U(dt)* produced by coaxial extrusion in transpressive systems as follows:

$$U(dt) = z(t_1) - z(t_0) = z(t_0)\,\delta\,[sin^2 \upsilon + cos^2 \upsilon \cdot exp(\dot{\varepsilon}t)] - z(t_0) =$$
$$z(t_0)\,\{\,\delta\,[sin^2 \upsilon + cos^2 \upsilon \cdot exp(\dot{\varepsilon}t)] - 1\} \qquad \text{(Eq. 1)}$$

where $z(t_0)$ and $z(t_1)$ are vertical distances to a reference level of zero extrusion (Rigid Floor Depth RFD, Schulmann et al., 2003) for times t_0 and t_1, respectively; δ is the true dip of the shear zone; υ is the angle between the extrusion direction of the coaxial component and the dip direction of the zone; $\dot{\varepsilon}$ is the coaxial strain rate and t is the time deformation has been acting (see Appendix A1 for a detailed reasoning).

https://doi.org/10.5194/egusphere-2025-538
Preprint. Discussion started: 25 February 2025

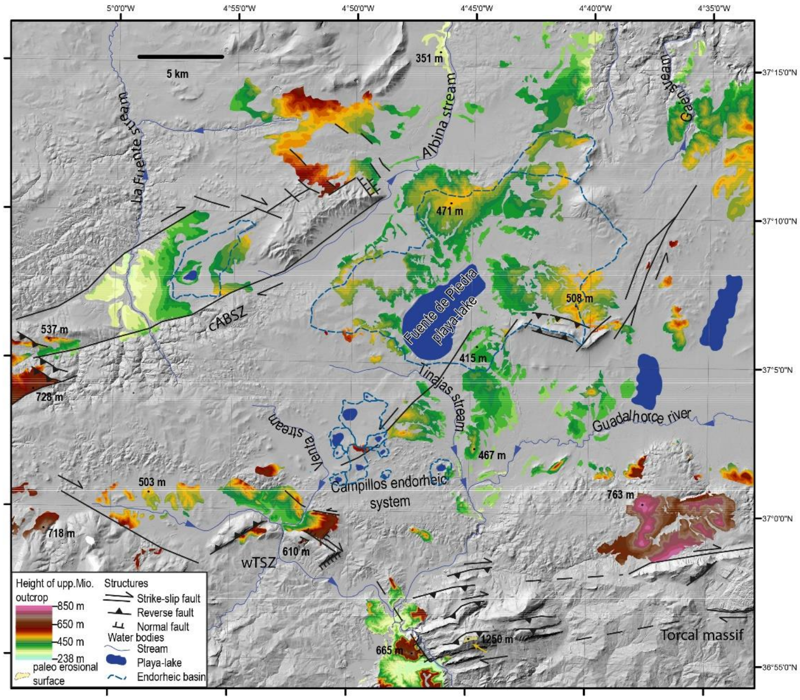

Fig. 3. Hillshade map that shows the altitude of upper Miocene shallow marine outcrops in the study area and main post-Serravallian structures. The area includes the ADA (Antequera Depressed Area), the ABSZ and TSZ (Algodonales-Badolatosa Shear Zone and Torcal Shear Zone, respectively). It should be noted that the lowest altitudes are located within the ADA, whilst the highest ones are located close to the main shear zones. The map also shows Atlantic streams (Albina, La Fuente and Gaén streams), Mediterranean streams (Venta, Guadalhorce and Tinajas streams) and main endorheic basins. See location in Fig. 2A (Junta de Andalucía, 2016).

3.2. Drainage network analyses and geomorphic indexes

For the analysis of the drainage network, we have interpreted key features of both the plan view geometry and the long profile of selected streams that cross the ABSZ. Within the Atlantic watershed, we have explored the Gaén stream, a Guadalquivir tributary that flows to the N (Figs. 2 and 3). Other Guadalquivir tributaries that have been studied in previous works have

https://doi.org/10.5194/egusphere-2025-538
Preprint. Discussion started: 25 February 2025

been also added to our interpretation: La Fuente and Albina streams (Fig. 3; Jiménez-Bonilla et al., 2023). For the Mediterranean watershed, we have focused on the la Venta and Tinajas streams, which are tributaries of the Guadalhorce river, which finally discharges into the Mediterranean Sea (Figs. 2 and 3). We displayed post-Serravallian structures on stream profiles to investigate the relationship between knick-points and recent structures. To better identify knick-points, we used the Stream Length-gradient index (SL), but normalized by the graded river gradient (k): We applied the SLk index, which quantifies differences in the gradient on profiles generated to either lithological or tectonic contrasts (Pérez-Peña et al., 2009).

$SL = (dh/dl) * L$ (eq. 2)

Where dh/dl is the slope and L the channel length. This index is normalized by k, graded river gradient:

$k = (C-hf) / \ln Lt$ (eq. 3)

Where C is the river head elevation, hf elevation in the river mouth and Lt the total length (Pérez-Peña et al., 2009). We fixed a horizontal distance of 250 m.

3.2.1. Analysis of playa-lakes and captures

The Fuente Piedra playa-lake and the Campillos endorheic system are studied in relation to their drainage network evolution, geometric changes and stream captures, which are potentially controlled by active tectonics. To do that, we delimited the average flooded surface (AFS) and the endorheic watershed (W) using a 5-m DEM from Junta de Andalucía. Paleo watershed (p-W) can be delimited by the presence of knickpoints along stream profiles, which are used as a part of the water divide (Fig. 4A). However, p-W are sometimes measured indirectly by the relationship between W and AFS. AFS and W, together with the average runoff estimated in each location are related, such that we use the ratio W/AFS as an approximation to the water balance of playa-lakes (e.g. Rodríguez-Rodríguez et al., 2012). Most playa-lakes in the Betics present similar W/AFS ratios (10-25), with slight variations attributed basically to differences in effective rainfall (ranging from 70 mm/year in the driest central part of Andalusia to 270 mm/year near the western

https://doi.org/10.5194/egusphere-2025-538
Preprint. Discussion started: 25 February 2025

Atlantic coast) and to local factors such as human modifications of the W, suggesting these systems share their main controlling parameters: permeability of the substrate, climatology and average runoff (Rodríguez-Rodríguez et al., 2007). Assuming a constant climate, W/AFS ratio should be maintained for each playa-lake. The DEM also allowed us to delimitate the paleo-Average Flooded Surface (p-AFS) of several playa-lakes that have reduced their size and even of those that are currently desiccated (Fig. 4A). Because of the flat topography of the playa-lakes, we have identified such p-AFS as a flat surface currently perched over the recent AFS. Once the p-AFS is calculated, the size of the p-W can be easily estimated.

3.2.2. χ index and divide migrations

Additionally, the Atlantic-Mediterranean water divide stability has been evaluated by means of the χ index, which permits to predict water divide movements by comparing the shape of streams long profiles situated on both sides of the water divide (Harkins et al., 2007; Perron and Royden, 2013; Willett et al., 2014). χ maps yield a measurement of the disequilibrium of stream channels in opposite basins respecting a divide given that the χ index depends inversely to the drained area. The χ-transformed profile of a river is defined by the following equation when uplift rate (U) and erodibility (K) in time and space are considered as constant:

$$z(x) = zb\ (xb) + \left(\frac{U}{K\ A_0^m}\right)^{l/n} \chi \quad \text{(eq. 4)}$$

With

$$\chi = \int_{xb}^{x} \left(\frac{A0}{A(x)}\right)^{m/n} dx \quad \text{(eq. 5)}$$

where z(x) is the elevation of the channel, x is the longitudinal distance, z_b is the elevation at the river's base level (distance x_b), A is the drainage area, A_0 is a reference drainage area, and exponents m and n are empirical constants.

Thus, χ mapping allows us to elucidate divide migrations when χ is compared across drainage divides: similar values on both sides of the divide suggest that two opposite streams are

https://doi.org/10.5194/egusphere-2025-538
Preprint. Discussion started: 25 February 2025

near equilibrium. If not, the stream with larger χ value for a given altitude tend to be captured by basins with lower χ (Willett et al., 2014; Fig. 4B). We made a χ map for the study area and we considered the discharge point at the sea level.

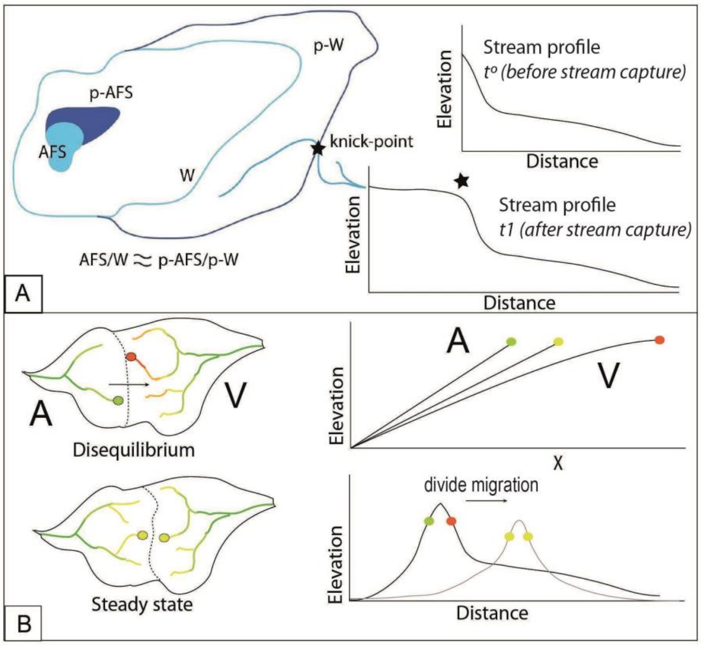

Fig. 4. (A) Methodology applied to study the evolution of playa-lake systems (AFS: Area Flooded Surface; p-AFS (paleo-Area Flooded Surface). (B) Diagrams of χ map showing the drainage network evolution when the water divide is in disequilibrium, stream profiles in χ space and water divide profiles changes from a disequilibrium to a steady state (A: Stream aggressor and V: Stream victim). Modified from Willett et al., 2014.

4. Results I: Post-Serravallian structures

https://doi.org/10.5194/egusphere-2025-538
Preprint. Discussion started: 25 February 2025

On the basis of previous works on the structure and kinematics of the TSZ and ABSZ, we have completed the structural record of these shear zones in the study area (Fig. 5). Additionally, we include for the first time kinematic data within the ADA.

4.1. Structures related to main shear zones (the ABSZ and the TSZ)

Our new structural data from the ABSZ come from the central ABSZ segment, which is the N boundary of the ADA (Figs. 2 and 3). To the SW, the central ABSZ oversteps the western ABSZ segment, being both linked by a restraining bend characterized by NW-SE oriented reverse faults (Figs. 5A and 5B). All these structures limit and deform WSW-ENE elongated sedimentary depocenters, upper Miocene to Quaternary in age (Figs. 3 and 5A). The deformation within the central ABSZ is partitioned into: (1) WSW-ENE to SW-NE dextral-normal faults (Fig. 5C) dipping up to 80º to the SE, (2) NW-SE dextral faults (Fig. 5C) interpreted as Riedel, which are particularly localized between the central and the eastern ABSZ.

https://doi.org/10.5194/egusphere-2025-538
Preprint. Discussion started: 25 February 2025

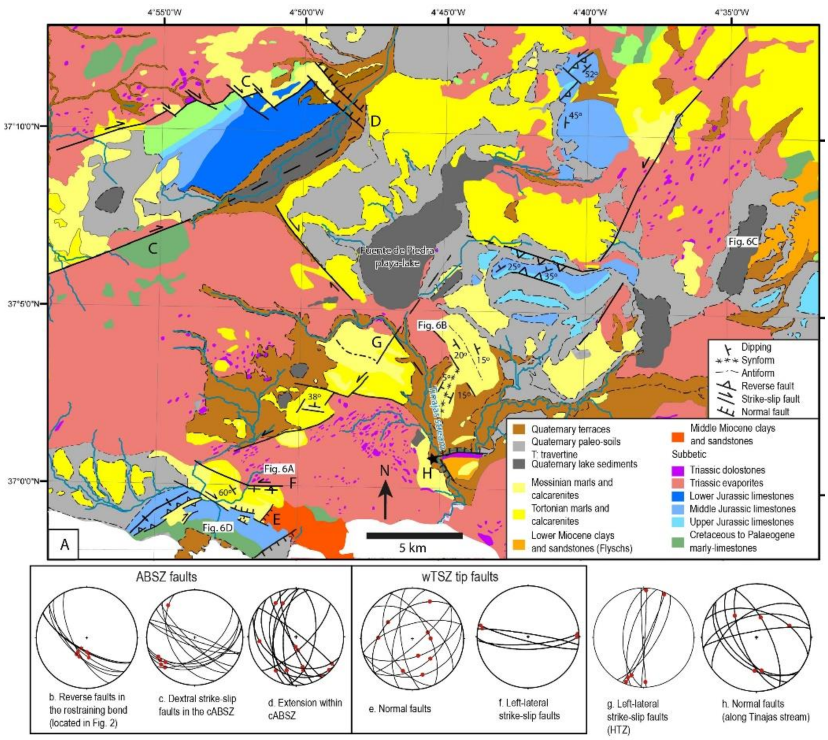

Fig. 5. (A) Geological map of the study area showing the main post-Serravallian structures of the ADA, the central ABSZ and the wTSZ. See Fig. 2A for location. (B), (C) and (D) Stereoplots related to structures of the ABSZ. (E) and (F) Stereoplots of structures in the W tip of the TSZ. (G) and (H) Stereoplots of structures within the ADA (Modified from Jiménez-Bonilla et al., 2023).

Within the TSZ, we collected new data from structures that deform the upper Miocene rocks located in the western TSZ (Figs. 3 and 5). At this site, Miocene rocks are gently folded by km-scale, WNW-ESE folds, and their limits are significantly determined by faults. Thus, normal faults often developed in the contact between the Miocene rocks and the Jurassic limestones (western TSZ, Figs. 3 and 5) as well as in its SE limit. They are defined, respectively, by WNW-ESE and NE-SW fault planes that usually dip between 50º and 80º (Figs. 5A and E). The high pitch of slickenlines (>60º) together with kinematic indicators, such as S-C structures, show a

https://doi.org/10.5194/egusphere-2025-538
Preprint. Discussion started: 25 February 2025

dominant normal dip-slip component. The WNW-ESE fault system also hosts Miocene rocks within grabens surrounded by Jurassic limestones. The NE boundary of the Miocene outcrop is controlled by steeply dipping, WNW-ESE left lateral faults, interpreted as a positive transpressive flower structure because of the subordinate reverse-slip component (Figs. 5F and 6A). The bedding within its deformation zone is nearly vertical or even overturned up to 60º (Fig. 5A). Gentle slickenlines pitch angles, lower than 10º, together with kinematic indicators show a left-lateral strike-slip movement (Figs. 5F and 6A). This fault zone also involves Jurassic limestones.

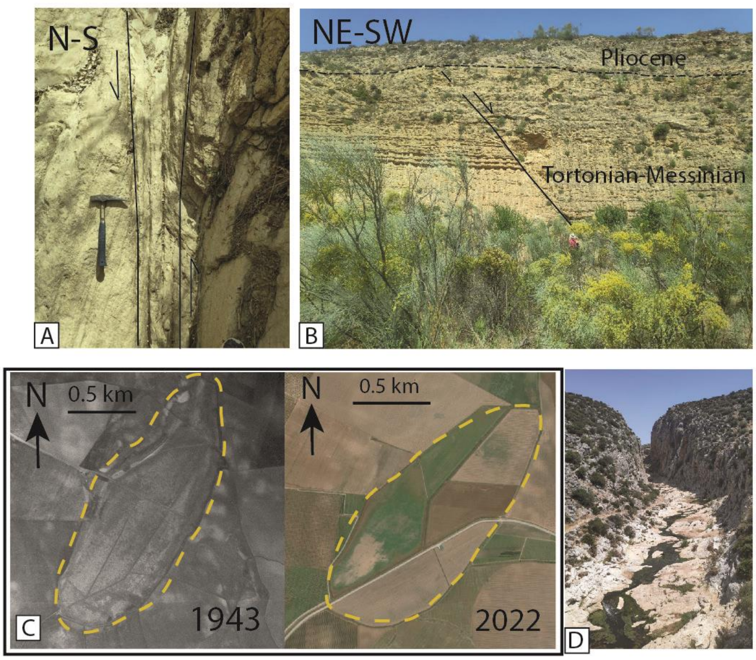

Fig. 6. Pictures of (A) vertical view of a left-lateral strike-slip fault zone that affect upper-Miocene rocks in the wTSZ, (B) a normal fault sealed by Pliocene sediments within the ADA, (C) aerial photographs to show the disappearance of a playa-lake due to human modifications (playa-lake is shown by discontinuous yellow line). PNOA images from 1943 and 2022 and (D) picture of the Venta stream deeply incised into the bed rock when it crosses the wTSZ. See location on Fig. 5A.

https://doi.org/10.5194/egusphere-2025-538
Preprint. Discussion started: 25 February 2025

4.2. Structures within the ADA

In the ADA, Jurassic limestones crop out as tectonic windows in scattered topographic highs (Fig. 5A). Moderately deformed upper Miocene rocks overlie Jurassic limestones and Triassic evaporites and claystones. The deformation observed in upper Miocene rocks within the ADA is less pervasive than in the TSZ and the ABSZ and it is localized in deformation bands.

The main post-Serravallian structure is a transverse zone formed by three different segments: two NNE-SSW left-lateral strike-slip fault zones linked by a WNW-ESE restraining bend (Fig. 5A). NNE-SSW deformation bands are more than 2 km long. They form semi-brittle, damage zones, more than 1 km wide, where they affect Triassic clays and evaporites, whilst they develop as discrete faults where they affect competent rocks (i.e. Jurassic limestones; Fig. 5A). Within the damage zones, dolostones bodies reorientate their long-axis to become parallel with the fault zone, as it occurs in other deformation bands within Triassic rocks (e.g. in the eastern ABSZ; Díaz-Azpiroz et al., 2020; Fig. 5A). Fault planes within the damage zones are highly dipping and slickenlines between 5º and 20º (Fig. 5G) indicates a dominant lateral movement. The western fault zone constitutes the SE boundary of the Fuente de Piedra playa-lake basin and separates it from another small playa-lake to the E, which is at the uplifted block in this sector (Fig. 5A). The restraining bend between both sinistral fault zones develops as a pop-up structure uplifted by WNW-ESE, kilometric-scale tight folds and NNE/SSW-dipping fault planes. Its eastern tip is dragged by the western sinistral fault zone (Fig. 5A). Some of the faults related to this transverse zone affect quaternary sediments.

In addition to the transverse zone, some dip-slip dominated, normal faults affect upper-Miocene and younger formations. These faults are not concentrated in long fault zones, but they are usually discrete faults up to 1 km long (Fig. 5A). Vertical throw related to these faults is estimated to be smaller than 200 m using upper Miocene markers. These faults show two orientations: NW-SE faults that throw down the SW block and WSW-ENE faults that descend the N block. Slickenlines show pitch angles higher than 45º and, together with kinematic

https://doi.org/10.5194/egusphere-2025-538
Preprint. Discussion started: 25 February 2025

indicators such as slickenfibers or S-C-like structures, indicate the downthrow of their hanging wall (Fig. 5H). The Fuente de Piedra playa-lake is in the N downthrown block of one of these WSW-ENE faults (Figs. 5A).

Additionally, some hm-hectometric-scale, open folds (interlimb angle larger than 120º) have been locally recognized (Fig. 5A). They are non-cylindrical folds, and their fold axis (NNW-SSE to NNE-SSW) are oblique to the Betic local regional orogenic grain (i.e., WSW-ENE).

5. Results II: Estimates of post-Tortonian differential surface uplift

As shown in section 4, faulting involves Tortonian formations. Additionally, these formations show noticeable altitude differences between the ABSZ, TSZ and the ADA, (from 250 m a.s.l to 850 m a.s.l.; Fig. 3). Main features are as follow:

(1) Upper Miocene deposits altitude varies generally between 450 and 550 m along the ABSZ. The highest altitudes are found in the restraining bend between the central ABSZ and the western ABSZ (728 m a.s.l.; Figs. 2A, 3 and 5B).
(2) In the TSZ, these sediments are located between 550 and 850 m. In the TSZ western segment, the highest altitudes are found in those affected by left-lateral strike-slip faults that build up a positive flower (up to 610 m a.s.l.; Figs. 3, 5A, 5F and 6A). Towards the E, in the central segment (north of the TSZ, see Fig. 3 for location), these deposits reach their maximum altitudes within this shear zone (850 m a.s.l.). A paleo erosional surface dated as upper Miocene (Lhénaff, 1977) is correlated with this Tortonian sea level and located at 1,200 m a.s.l. (Barcos et al., 2015; Fig. 3).
(3) The highest altitudes in the ADA are found in the restraining bend of the above-described transverse zone (upper Miocene sediments up to 500 m a.s.l.), whereas undeformed areas would be at 350 m a.s.l. (Fig. 3).

Therefore, the post-Tortonian differential surface uplift (in the sense of England and Molner, 1990) at the main shear zones compared to the endorheic basins in the less deformed areas would

https://doi.org/10.5194/egusphere-2025-538
Preprint. Discussion started: 25 February 2025

reach around 200 m at the ABSZ, whereas at the TSZ is more than 350 m. Considering their spatial relationship and differences on Tortonian deposits altitude, we hypothesize that the recent deformation at these two shear zones is responsible for the observed differential uplift.

To test this hypothesis, we estimated the theoretical surface uplift produced by post-Tortonian transpressional deformation at the TSZ, following the approach of Schulmann et al. (2003) and Fuentes et al. (2019). The data needed for these calculations were obtained from previous detailed studies on the kinematics of this shear zone (Díaz-Azpiroz et al., 2014; Barcos et al., 2015) and are presented as follows (see also Table 1): (1) According to geophysical data, the base of the Triassic layer, where the main detachment (i.e., rigid floor depth, RFD, in Schulmann et al. ,2003) would be located, is between 4500 and 6000 m (see also Medialdea et al., 1986 and Torné et al., 1992). We assume that the vertical distance of the analyzed formations to the RFD at the onset of deformation $z(t_0)$ equals these values. (2) The true dip of the shear zone (δ) is 73ºN. (3) Coaxial deformation is assumed to be pure shear and the extrusion angle (υ) is 0º ± 5º, thus we consider up-dip pure shear (υ = 0º), such that Eq. 2 simplifies to the Schulmann et al (2003) specific case:

$$U(dt) = z(t_0)\,[(\dot{\varepsilon}t)\ - 1] \qquad \text{(Eq. 6)}$$

The pure shear strain rate ($\dot{\varepsilon}$) is obtained from the total contraction accommodated orthogonally to the shear zone along a specific time interval (t) $e\ = \frac{\dot{\varepsilon}}{t}$, which results in $\dot{\varepsilon}\ =\ e\,t$. The onset of transpressional deformation at the TSZ needs to be younger than chevron folds that affected Upper Cretaceous-Paleogene reddish marly limestones of the Subbetic units, since these are interfered by transpressional structures (Díaz-Azpiroz et al., 2014). The age of these folds spans from 20.4 Ma (Aquitanian-Burdigalian boundary), since the youngest deposits affected by these folds are Aquitanian in age, to 11.6 Ma (Serravalian-Tortonian boundary; Expósito et al., 2012). The total contraction produced at the inner domain of the Torcal de Antequera massif of the TSZ

https://doi.org/10.5194/egusphere-2025-538
Preprint. Discussion started: 25 February 2025

along this interval ranges from 0.2 (obtained from cross-sections) to 0.27 (calculated from asymmetrical fold geometry). From these values, the resulting average pure shear strain rate related to transpression that acted in the TSZ in the last 11.6-20.4 my ranges between $3.2 \cdot 10^{-16}$ s-1 and $7.4 \cdot 10^{-16}$ s-1. (4) The transpressional deformation that affected the upper Miocene calcirudites and calcarenites should have begun after the Tortonian, say in the Tortonian-Messinian transit, 7.3 my ago. If we assume the strain rate remains roughly constant, we can calculate the total contraction (e), which is equivalent to the product $\dot{\varepsilon}\, t$ = 0.07 – 0.17. By substituting all these data into Eq. 2, we obtained the range of the tectonic uplift U(dt) due to transpressional deformation at the TSZ in the last 7.3 my (167 - 868 m, Table 1 and Fig. 7), depending on the RFD depth and the total contraction (e). Our differential uplift estimations based on the current altitudes of the post-Tortonian marine sediments are better reproduced considering a total contraction value (e) between 0.09 and 0.11 (for any RFD value). Different combinations of RFD with e = 0.07-0.09 (large RFD) or e = 0.11-0.15 (small RFD) may also produce reasonable correlations. Contraction values larger than 0.15 or lower than 0.07 would not explain the observed uplift results.

Table 1. Input data used for the modelling of post-Tortonian tectonic uplifting due to transpression at the TSZ (from Díaz-Azpiroz et al., 2014 and Barcos et al., 2015) and results of this model. z(t1) is the vertical distance to the RFD for time t1 (after deformation) and U(dt) is the corresponding uplift. See the main text for further details.

Factor	**Input data**
$z(t_0)$	4500 – 6000 m
δ	73º
υ	0º

$\dot{\varepsilon}$	$3.2 \cdot 10^{-16} - 7.4 \cdot 10^{-16}$ s^{-1}
t	7.3 my
$e = \dot{\varepsilon}t$	0.07 – 0.17
	Results
$z \quad (t_1)$	4615 – 7368 m
$U(dt)$	167 – 868 m

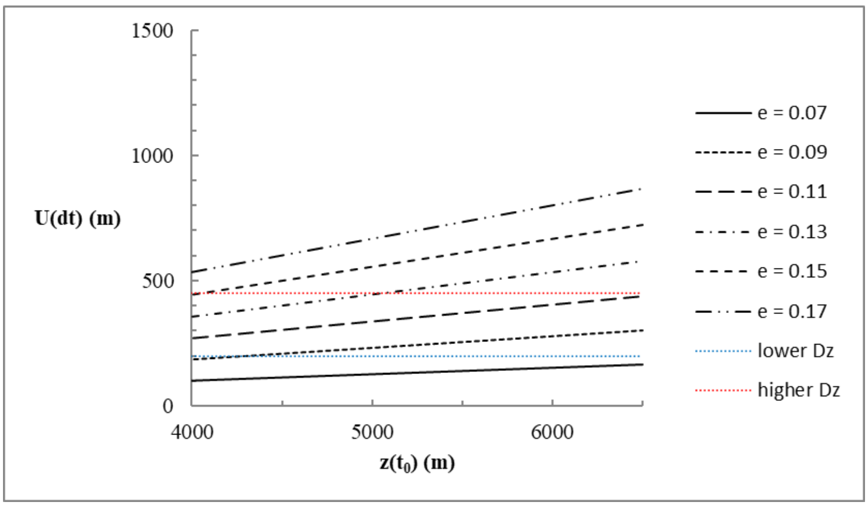

Fig. 7. Theoretical post-Tortonian tectonic uplift due to the coaxial component of transpressional deformation at the TSZ versus the RFD for different possible total contraction values (e), as calculated from kinematic models. The range of differential uplift measured between the current altitude of Tortonian deposits at the TSZ and at the neighbouring undeformed area (Dz) is also shown for comparison.

https://doi.org/10.5194/egusphere-2025-538
Preprint. Discussion started: 25 February 2025

6. Results III: Geomorphic results

Geomorphic results are derived from the analysis of streams (stream long profile together with SLk index) that drain part of the ADA and flow to the Mediterranean Sea or to the Atlantic Ocean (Figs. 1 and 2) or the playa-lakes located at the centre of some endorheic areas (Figs. 8 and 9). Table 2 compiles the information of changes of AFS and watersheds area and the relationships between both. We have identified 17 endorheic basins with playa-lakes at their centre that developed during the last 3,000 years. Three of them (numbers 14, 15 and 16 in Table 2) were discarded from the analysis because their water balances are influenced by human modifications of the AFS and W, such as drainages (AFS) and/or the construction of roads through them (W).

Table 2. Watershed (W), Average Flooded Area (AFS) and the W/AFS relationship of the 17 endorheic basins detected in the studied area currently and in the past (p-W, p-AFS and pW/AFS). Playa-lakes are located in Fig. 9 by numbering.

	W	AFS	W/AFS	p-W	p-AFS	p-W/p-AFS
1	1198.7 hm²	43.3 hm²	27.7	3328.1 hm²	135.2 hm²	24.6
2	0 hm²	0 hm²	-	4786.4 hm²	878.34 hm²	5.5
3	14116.4 hm²	1271.6 hm²	11.1	15846.26 hm²	1918.46 hm²	8.3
4	573.9 hm²	50.7 hm²	11.3	1271.4 hm²	95.7 hm²	13.3
3,2	26.2 hm²	1.3 hm²	20.2	0 hm²	0 hm²	-
5	153.9 hm²	39.9 hm²	3.9	264.4 hm²	39.9 hm²	6.6
6	26.4 hm²	1.5 hm²	17.6	322.1 hm²	33.4 hm²	9.6
7	82.7 hm²	9.3 hm²	8.9	82.7 hm²	9.3 hm²	8.9
8	53.8 hm²	5.6 hm²	9.6	53.8 hm²	5.6 hm²	9.6
9	241.5 hm²	12.1 hm²	20.0	181.2 hm²	12.1 hm²	15.0
10	65.7 hm²	8.9 hm²	7.4	125.2 hm²	8.9 hm²	14.1

https://doi.org/10.5194/egusphere-2025-538
Preprint. Discussion started: 25 February 2025

11	19.6 hm²	5.1 hm²	3.8	359.1 hm²	15.2 hm²	23.6
12	0 hm²	0 hm²	-	174.5 hm²	15.6 hm²	11.2
13	172.5 hm²	16.2 hm²	10.6	0 hm²	0 hm²	-
14	0 hm²	0 hm²	-	7456.7 hm²	421.6 hm²	17.7
15	0 hm²	0 hm²	-	9310.0 hm²	549.6 hm²	16.9
16	797.5 hm²	22.9 hm²	34.8	797.5 hm²	42.3 hm²	18.9
17	0 hm²	0 hm²	-	7661 hm²	987 hm²	7.8

The χ map shows significant contrasting values across the Atlantic-Mediterranean water divide (Fig. 8). Guadalhorce tributaries are characterized by very low values at their headwaters ($\chi < 12.5$ m) whilst Guadalquivir tributaries always show $\chi > 20$ m at their headwaters.

https://doi.org/10.5194/egusphere-2025-538
Preprint. Discussion started: 25 February 2025

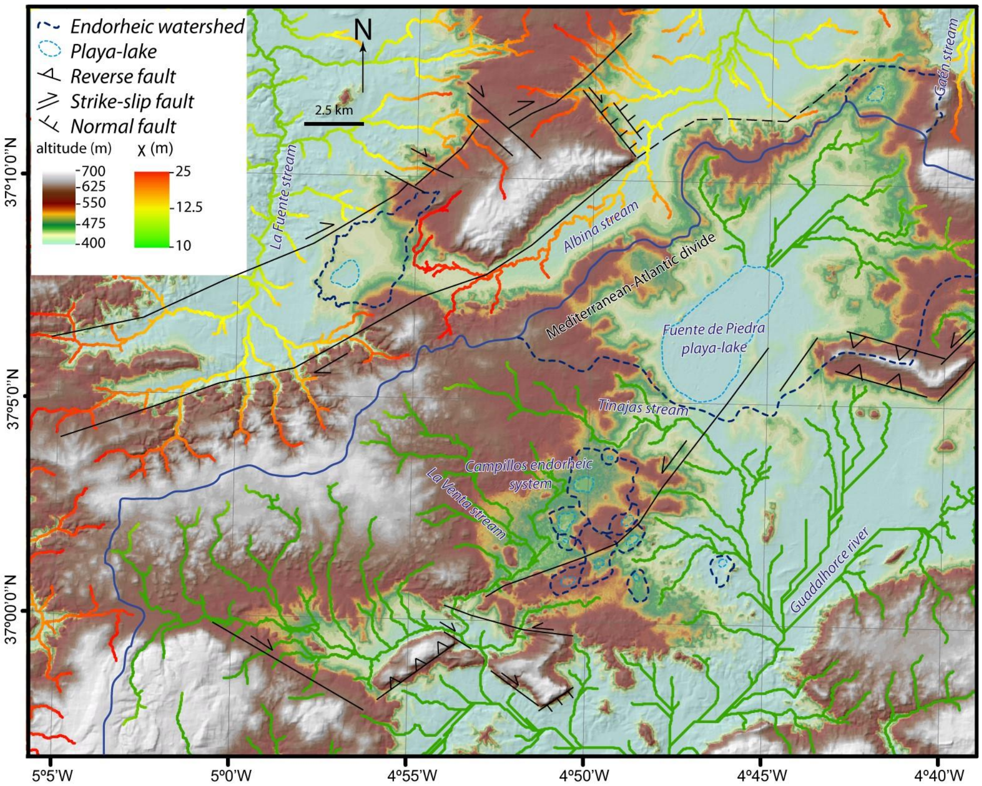

Fig. 8: χ map together with the DEM showing the main playa-lake systems and post-Serravallian structures (Junta de Andalucía, 2016; modified from Jiménez-Bonilla et al., 2023). See location in Fig. 2.

Regarding the Atlantic watershed, previous studies analysed the captures of basins 1 and 2 by the Albina stream and La Fuente stream (Jiménez-Bonilla et al., 2023; Figs. 8 and 9). In order to complete the analysis of this watershed, we have performed the long profile and the SLk index for the Gaén stream (Figs. 9 and 10A). The long profile shows two different stream segments: a concave segment, which extends for approximately 5 km from the source, and a slightly convex profile with a higher gradient, located downstream. Both stream segments are separated by a knick-point, higher than 20 m, that is related to a SLk value greater than 15 (Fig. 10A).

https://doi.org/10.5194/egusphere-2025-538
Preprint. Discussion started: 25 February 2025

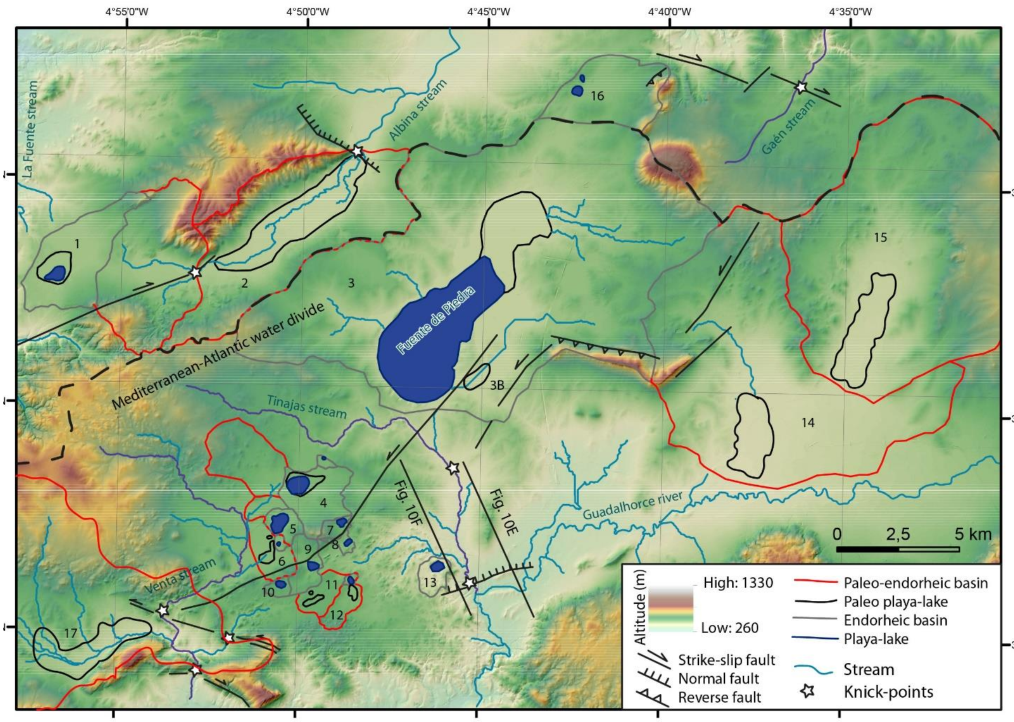

Fig. 9. Relief map of the ADA that shows the development of the studied playa-lakes and their related watershed. Location is the same as Fig. 5A. (Junta de Andalucía, 2016).

https://doi.org/10.5194/egusphere-2025-538
Preprint. Discussion started: 25 February 2025

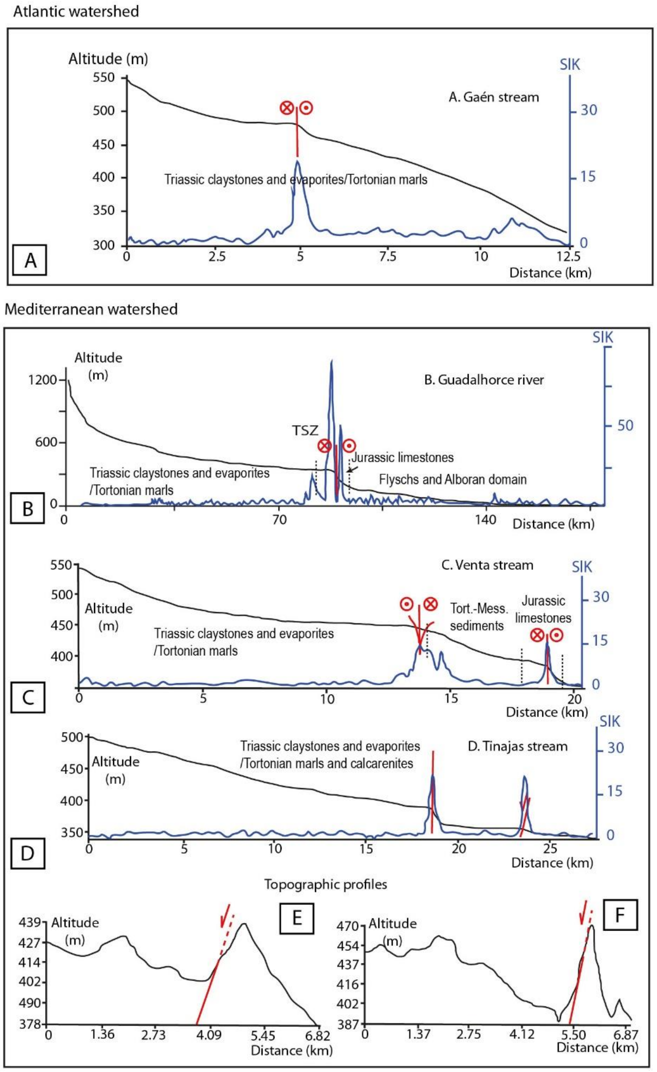

Fig. 10. (A), (B), (C) and (D) stream and SlK profiles of main rivers of the Atlantic (Gaén stream) and Mediterranean (Guadalhorce, Venta and Tinajas stream) watersheds within the studied area. (F) and (G) topographic profiles parallel to the Tinajas stream. See Fig. 9 for location of streams.

In general, Mediterranean streams frequently show steeper gradients than Guadalquivir tributaries. In the studied area, the main Guadalhorce river exhibits an elbow geometry in plan view (Figs. 1 and 2). Two kilometers downstream of the elbow there is a knick-point and an SlK

https://doi.org/10.5194/egusphere-2025-538
Preprint. Discussion started: 25 February 2025

value of more than 75, which is related to the capture of the upper Guadalhorce watershed (at 85 km from the source; Fig. 10B). The Guadalhorce segment that runs through the ADA, upstream of the Guadalhorce capture, shows a flat stream long profile and it flows on thick alluvial deposits (Figs. 5A and 10B). Downstream of the knickpoint, the stream profile shows a steeper gradient, and the river is deeply incised into the limestones of the TSZ.

More in detail, we also analyse the Tinajas and the la Venta streams (Figs. 10C and 10D), which discharge in the Guadalhorce river upstream of its capture (Figs. 1, 2 and 9).

The La Venta stream is an antecedent river that crosses perpendicularly the western TSZ (Fig. 2A, 6D and 9). Its long profile is characterized by the presence of two knickpoints, located at 13 and 19 km, which show SLk values higher than 10 (Fig. 10C). The La Venta stream shows a concave profile from its source down to the first knick-point. This knick-point spatially coincides with two post-Tortonian fault zones (Figs. 5A, 6A and 10C). The stream segment between both knick-points shows a higher slope and it is characterized by a gorge deeply incised into the Jurassic limestones of the western TSZ (Fig. 6D). The knick-point located at 19 km is related to a post-Tortonian dextral strike-slip fault. This knick-point builds up a waterfall > 10 m high (Fig. 10C) with an associated 5-10 m thick tufa outcrop, located at 420 m a.s.l., and dated at 9,000 BP (Comino and Senciales, 2012). Additionally, there are many cavities in the Peñarrubia range that worked as phreatic conducts. These conducts are currently preserved upper than 100 m from the phreatic surface, within the vadose zone, thus supporting the hypothesis of the recent uplift of the western TSZ.

To the E of the La Venta stream head there are 9 playa-lakes (endorheic basins 4 to 12; Fig. 9 and Table 2) that constitute the Campillos endorheic system. Playa-lakes 4, 6, 11 and 12 show a significant decrease on their AFS during the Pleistocene to Holocene, which is related to water input reduction because of W reduction, as suggested by roughly constant W/AFS ratios (Table 2). Other playa-lakes increased their W and AFS (e.g. playa-lake 9: Fig. 9 and Table 2). By contrast, W and AFS pairs of playa-lakes 7 and 8 remained steady during the last thousands

https://doi.org/10.5194/egusphere-2025-538
Preprint. Discussion started: 25 February 2025

of years (Fig. 9 and Table 2). To the W of the La Venta stream we have mapped the paleo playa-lake 17. It is a depressed area with a flat topography and filled by moor sediments.

From headwater to mouth, the Las Tinajas stream changes its trend from W-E to NW-SE and finally to N-S close to the mouth (Fig. 9). The stream profile also shows two knickpoints close to the mouth: at 19 and 24 km, which show SLk values higher than 15 (Fig. 10D). As the La Venta stream, it shows a concave geometry from the source down to the first knick-point (Fig. 10D). This stream segment is characterized by low erosion rates (concave stream segment) and thick quaternary alluvial terraces. The biggest playa-lake in this area, the Fuente de Piedra playa-lake, is only 800 m to the N of this stream segment (playa-lake 3). Although the W sector of this playa-lake seems to remain steady during the Holocene, its AFS was likely reduced (from approx. 1900 hm2 to 1300 hm2; Fig. 9 and Table 2). From 19 to 24 km the stream profile shows a flat geometry and alluvial terraces were deposited during the Holocene. Close to this stream segment the playa-lake 13 developed (Table 2 and Fig. 9). The knick-point located at ca. 24 km spatially coincides with normal faults previously described (Figs. 5A, 5E and 9). This knick-point is also associated with a gorge, > 5 m high (Fig. 10D). When topographic profiles are drawn parallel to the stream profiles, we observe that this knick-point is associated with a topographic escarpment SW-NE (Figs. 9, 10E and 10F).

Endorheic basins 14 and 15 developed along the Guadalhorce river right bank, upstream of the Tinajas stream outlet (Fig. 9 and Table 2). Although they are currently drained by a channel network used for agriculture purposes, endorheic basin 14 was captured by the Guadalhorce during the Holocene whilst endorheic basin 15 was not.

7. Discussion

To understand the birth of internally drained basins and the Atlantic-Mediterranean watershed divide migration is important to identify the mechanisms that controlled the upper Miocene differential surface uplift and how it controls the recent evolution the Western Gibraltar Arc. Our results will be put in context together with data from previous works that account for some of these processes.

7.1. Role of transpressional tectonics on the ADA inception

First evidence of emersion in the study area dates from the upper Miocene. The upper Miocene coastline has been mapped in previous works by detecting Tortonian and Messinian abrasion platform borders (Elez et al., 2016; Braga et al., 2003; Fig. 11). Its current position shows that the central TSZ was probably uplifted at the late Tortonian more than 500 m above the sea level. This uplift was probably favoured by the transpressional activity at this zone. However, depressed parts of this barrier, associated with relay zones between shear zone segments, likely allowed to localize the Atlantic-Mediterranean communication through the Guadalhorce gateway (Figs. 1 and 11). The activity of the TSZ along the Messinian continuously raised this topographic barrier, finally closing the Guadalhorce gateway at 6.2 My (Fig. 11). This, together with the closure of the other gateways between the Atlantic Ocean and the Mediterranean Sea, isolated the latter (Roveri et al, 2014). Because of its negative water balance, the sea level in the Mediterranean Sea sharply dropped more than 1000 m, giving place to the Mediterranean Salinity Crisis (MSC; Martín et al., 2001; Blanc, 2006; Madof et al., 2019), whilst the sea level in the Atlantic watershed maintained. This is illustrated by the Mediterranean stream incision on upper Miocene outcrops that originated deep gorges in the Messinian (Elez et al., 2016; 2020). Despite the high stream power erosion of Mediterranean streams, this divide remained stable at the TSZ until the Pliocene (Elez et al., 2016 and this work), probably due to the Messinian tectonic activity of the TSZ as we have observed in this work. Instead, the Mediterranean Sea reopened to the Atlantic by means of the Gibraltar strait, which provoked the Zanclean flood at 5.33 My (Roveri et al., 2014) and the levelling of both watersheds. This opening was probably favoured by the existence of E-W trending faults located in the strait area (Luján et al., 2011).

https://doi.org/10.5194/egusphere-2025-538
Preprint. Discussion started: 25 February 2025

There is consensus about the importance of post-Tortonian uplift in the western Betics. Previous works , based on geomorphology models, attributed 50-55% of the upper Miocene uplift (or all post-Messinian uplift) observed in the Guadalhorce watershed to an isostatic rebound, produced by differential erosion rates between Atlantic and Mediterranean watersheds provoked by the sea level drop in the Mediterranean watershed, a direct consequence of the MSC (Farines et al., 2015; Elez et al., 2016, 2020). However, according to the model assumptions, these estimations are valid in the orogen-scale but do not consider differential uplifting at different sectors and/or specific structures within the Atlantic-Mediterranean divide area. The results presented here in combination with some of our previous works (Díaz-Azpiroz et al., 2014; Barcos et al., 2015) fill this gap. In the study area, Tortonian-Messinian sediments, deposited close to the sea level, were uplifted up to 610 m in the western segment of the TSZ and up to 850 in the central TSZ (part of the current Mediterranean watershed; Fig. 3). These are 200-450 m higher than the same sediments in the ADA. This range contains theoretical post-Tortonian uplifting values calculated through a transpressional kinematic model using specific combinations compatible with the TSZ activity (Fig. 7). Therefore, our results indicate that transpression at the TSZ with moderate strain rate values (likely resulting in total contraction between 0.09 and 0.11), roughly constant since the Messinian, would suffice to explain the observed differential uplift with respect to the depressed sector of the study area. Moreover, our structural results do not account for the elongate domal structure required by Elez et al. (2016, 2020) models.

In contrast with irrelevant uplift values reported previously for the Atlantic watershed (Elez et al., 2016; 2020), we also observed significant uplift in this watershed, especially related to the ABSZ. The differential surface uplift of the ABSZ compared to less deformed areas in the ADA would reach around 200 m. Unlike the TSZ, which partially emerged during the Tortonian, there is no evidence of ABSZ emersion until the Messinian (Elez et al., 2016). There are indeed Messinian sedimentary depocenters within the ABSZ (Fig. 5A, see also Jiménez-Bonilla et al., 2015). However, the current relief shows that some segments of the ABSZ reach 750 m (Fig. 9). These arguments suggest that the ABSZ tectonic activity, although kinematically similar to that

https://doi.org/10.5194/egusphere-2025-538
Preprint. Discussion started: 25 February 2025

of the TSZ, would start later. This is congruent with a diachronic migration of the deformation towards the foreland during fold-and-thrust belts evolution (e.g. Davis et al., 1983). Once the ABSZ emerged, the ADA individualized (Fig. 11). The age of the complete emersion of the ADA is not completely constrained. First homogeneous continental deposits (Pliocene conglomerates) overlay Messinian sediments, so emersion should have occurred at some point within the Pliocene (from 5 to 2.5 My). Moreover, first lake sediments, which are probably related to endorheic basins, are Pliocene in age (Medina 1991).

Both the TSZ and ABSZ accommodate the western Gibraltar arc protrusion, which is still active (Balanyá et al., 2012). The presence of earthquakes close to the ABSZ (e.g. Ruíz-Costán et al., 2012; Díaz-Azpiroz et al., 2022) and geomorphic analyses in the ABSZ and TSZ (e.g. Barcos et al., 2015; Jiménez-Bonilla et al., 2015 and this work) suggest that both shear zones are still active.

Consequently, although we do not discard a moderate post-Messinian uplift on the Mediterranean watershed, especially south of the TSZ, due to an isostatic rebound, our work highlights the importance of dextral transpressional bands on the generation of differential uplift within the fold-and-thrust belt (even in the Atlantic watershed).

https://doi.org/10.5194/egusphere-2025-538
Preprint. Discussion started: 25 February 2025

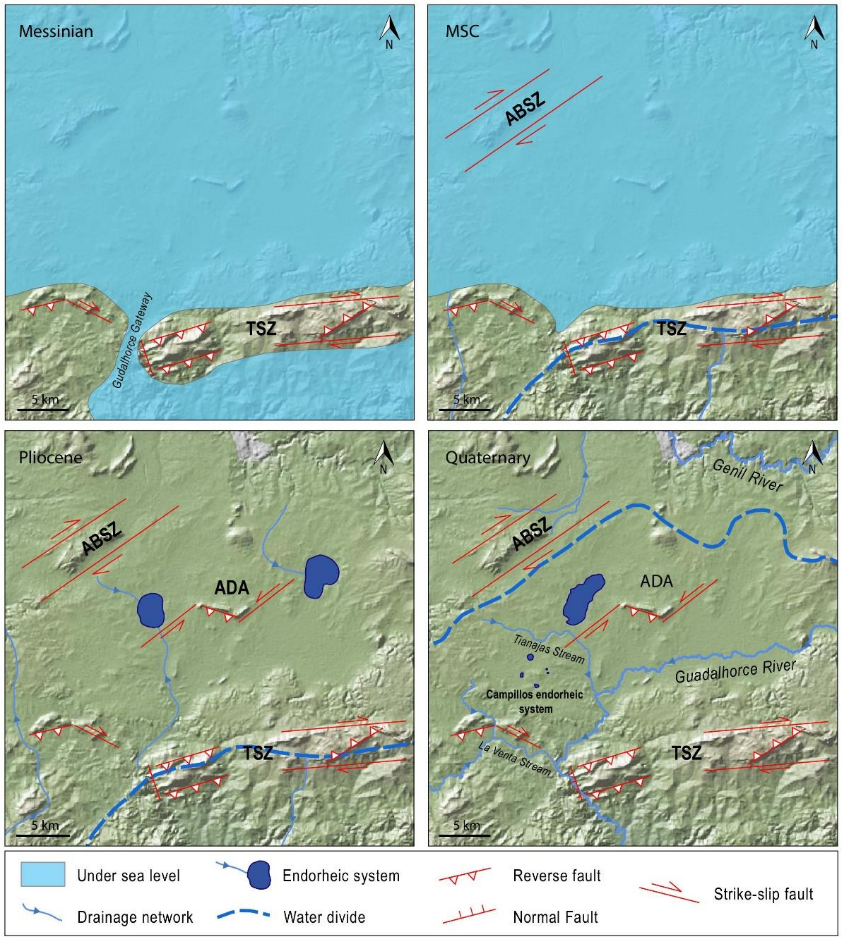

Fig. 11. Block diagram of the ADA inception and evolution (same area as in Fig. 3). We show the drainage network, water divide, mountain building and endorheic watershed evolution from Messinian to Quaternary (Junta de Andalucía, 2016).

7.2. Atlantic-Mediterranean water divide migration and the development of endorheic watersheds

The Atlantic-Mediterranean water divide originated during the Messinian Guadalhorce gateway closure, and was coincident with the TSZ (Figs. 2 and 11). This water divide must have

https://doi.org/10.5194/egusphere-2025-538
Preprint. Discussion started: 25 February 2025

been maintained close to the TSZ during the ADA continentalization as indicated by the Pliocene sediments north of the wTSZ: The source of these Pliocene conglomerates is the Alboran domain, which is farther S nowadays. It means that during the Pliocene, the flow direction was from the Alboran domain to the N, thus suggesting that this area was drained by Atlantic rivers. Nowadays, this area belongs to the Mediterranean watershed (From 5 to 1 My; Figs. 1, 2 and 5A). To the E of the ADA, there are some Pliocene lacustrine deposits (Medina, 1991; Vera, 2004). Consequently, endorheic watersheds were probably established since the ADA formed and they were close to the Atlantic-Mediterranean water divide at the Pliocene (Fig. 11).

The water divide would have therefore migrated NW-ward during the Quaternary (Figs. 2 and 11). This migration coincides spatially and temporarily with the outward propagation of the transpressive deformation front, accommodated by the ABSZ and TSZ. The Mediterranean capture of the ADA by the Guadalhorce river and its tributaries was probably favoured by the ABSZ related surface uplift, that blocked other northward possible captures, and the coeval NW-SE normal faults within the TSZ that depressed specific, narrow zones, such as those near the Guadalhorce course (Barcos et al., 2015).

Going to the recent evolution of the ADA, a crucial question is the evolution of current playa-lakes close to the Atlantic-Mediterranean water divide. Playa-lakes stricto sensu, as we described in sections 1 and 2, probably developed during the Early Pleiostocene, but due to their ephemerous lifespan, they disappeared or/and were reshaped and their sediments probably eroded. The earliest age obtained for current playa-lakes associated with endorheic basins is of 30 ky in the Fuente de Piedra playa-lake (Late Pleistocene; Höbig et al., 2016). Previous works have pointed out that since endorheic systems were formed, they were strongly conditioned by climatic changes and human modifications because of their weak equilibrium between water inputs and outputs (Rodríguez-Rodríguez et al., 2007; 2012). As we observed, the large number of playa-lakes preserved in the ADA is probably favoured by the most recent uplifts caused by both the TSZ and ABSZ and their respective tip zones, which shaped a roughly triangular closed zone that contains all the studied cases (see sections 4 and 5; Fig. 2) and act as relief barriers that prevent erosion from the Atlantic and Mediterranean streams (Fig. 2). Additionally, active tectonics in this sector may also influence the shrinkage or disappearance of some endorheic watersheds hosting playa-lakes because of the reduction of the overall water input due to stream captures (Figs. 3, 9 and Table 2; Jiménez-Bonilla et al., 2023).

The long lifespan of some playa-lakes such as Fuente de Piedra (30 Ky; Höbig et al., 2016) is probably conditioned by active tectonics. The dip-slip movement of the left-lateral dominated fault of the transverse zone within the ADA (see section 4.3) located at the E boundary of this playa-lake could have prevented this playa-lake capture, despite being located only about 1 km away from the upper course of the Las Tinajas stream, a tributary of the Guadalhorce (Table 2 and Fig. 5A; see also χ values on Fig. 8 and Fig. 9). Moreover, the Fuente de Piedra paleo-AFS would be bigger and it would include playa-lake 3B and 3 (Fig. 9 and Table 2). This left-lateral dominated fault would have splitted the playa-lake into two. The eastern one (playa-lake 3B) is separated by a topographic high with respect to its parental lake and it is located at 5 m higher than the current Fuente de Piedra bottom lake (Table 2 and Fig. 9).

In contrast, some playa-lake systems are the result of this recent activity, as the playa-lake 13, nucleated on the downthrown, northern wall of a WSW-ENE normal fault intersecting the lower course of the Las Tinajas stream (Fig 9). This stream is deeply incised into the bedrock in the uplifted southern wall of that fault.

Regarding the Campillos endorheic system (playa-lakes 4 to 12), its evolution seems to be conditioned by the balance between the western TSZ segment uplift and the headward erosion capacity of the La Venta stream. Although the La Venta stream is an antecedent river, as indicated by its strong incision (Fig. 6D), its upper course could have been transiently disconnected from the drainage network due to the uplift of western TSZ during the Quaternary. This disconnection probably formed an endorheic area where the Campillos endorheic system and paleo playa-lake 17 developed (Fig. 9 and Table 2). The age of this endorheic basin development is not well constrained. Nevertheless, the age of the travertine associated with the wTSZ uplift (9,000 years old, see section 6) must pre-date the recapture of playa-lake 17 as well as part of the paleo-playa-lakes of the Campillos endorheic system (Table 2). The partial preservation of this system would be due to the recent activity of a left-lateral dominated transpressive fault, located to the NE of the western TSZ. This fault together with all the structures related to this tip generate a relief barrier which slows down the migration of the knick-point upstream (Fig. 10C). It is also congruent with the relative uplift observed in the upper Miocene rocks of the western TSZ with respect to the ADA (Fig. 3). If the tectonic activity stopped at the western TSZ, the Campillos endorheic system would likely be captured in some hundred years. Other partial or complete captures of endorheic watersheds have been observed N of the Campillos endorheic system during the last 2,000 years (playa-lakes 1 and 2; Table 2; Recio-Ruíz and Ruiz-Somavilla, 1990; Jiménez-Bonilla et al., 2023). In this case, an Atlantic watershed river completely captured playa-lake 2 and partially playa-lake 1 because of the active tectonics of central ABSZ (Jiménez-Bonilla et al., 2023; Table 2; Fig. 9).

Although predictions of the future development of playa-lakes is speculative, some guidelines can be made. Mediterranean streams are aggressor streams, so they should capture part of endorheic basins and even Atlantic streams according to their lower χ values (Fig. 8). However, Mediterranean streams show really low incision capacity at their headwaters showing thick river terraces, open valleys and poor development of their drainage networks. The presence of knick-points along stream profiles is frequently favoured by active discrete faults that provoke relative uplift. Thus, although the Atlantic-Mediterranean water divide will probably move NW-ward, endorheic basins will develop, hosted between the ABSZ and the TSZ, within the ADA (Figs. 5, 8. 9 and 11). This work shows the study of a water divide movement and drainage integration of endorheic basins settled in a transpressional tectonic setting, which is complementary with previous works made in other tectonic settings: extensional settings (Repasch et al., 2017; Berry et al., 2019), foreland basins (Anton et al., 2014), intramontane basins (Giano and Schiattarella, 2023) and contractional belts (Sobel et al., 2003; Willett et al., 2014).

8. Conclusions

https://doi.org/10.5194/egusphere-2025-538
Preprint. Discussion started: 25 February 2025

In this work, we study a depressed area (ADA), limited by the TSZ and the ABSZ, to the S and to the N, respectively, within the Betics fold-and-thrust belt to delve into the Atlantic-Mediterranean water divide evolution from the Messinian to the Quaternary. This water divide is currently diffuse, and it is characterized by the presence of many endorheic watersheds. We combined structural and hydro - geomorphic analysis: we collected kinematic data from faults active during the last 5 My and we analysed the drainage network and endorheic watersheds using geomorphic indexes such as SLk and χ.

We observed differences on the post-Tortonian surface uplift within the study area that are congruent with the tectonic activity of both the TSZ and the ABSZ. Consequently, structures must be considered in studies of orogenic uplift in the Betics. The relative uplift built up by these shear zones condition the relief evolution and the drainage network development:

- The early uplift of the TSZ probably conditioned the Guadalhorce gateway closure and it did not reopen even though the high erosion power of Mediterranean streams during the Messinian Salinity Crisis (MSC). The TSZ uplift controlled the location and geometry of the Pliocene Atlantic-Mediterranean water divide.
- The ABSZ tectonic activity would start later than the TSZ, which suggests a migration of the deformation towards the foreland at this fold-and-thrust belt segment. This migration of the deformation probably conditioned the Quaternary migration of the Atlantic-Mediterranean water divide.
- The tectonic activity of both transpressive zones (the TSZ and the ABSZ) generated the ADA, where many endorheic watersheds develop from the Pliocene to Holocene. The recent tectonic activity of faults associated with TSZ and ABSZ prevents the capture of these endorheic watersheds from streams, especially those draining to the Mediterranean Sea. The kinematics of active faults may condition the evolution of playa-lakes (movement, split, diminution or increase of its average flooded area).

Author contributions

https://doi.org/10.5194/egusphere-2025-538
Preprint. Discussion started: 25 February 2025

AJB led the research and wrote the draft. AJB and MDA made analyses. MDA, AJB, MRR, IE, JLY and JCB participated in the fieldwork for both qualitative geomorphological analysis and structural analysis. All the authors participated in the results interpretation and in the text improvement.

Competing interests

The contact author has declared that none of the authors has any competing interests.

Acknowledgements

We thank the keepers of the Natural Reserve of Lagunas de Campillos and Fuente de Piedra for support during field surveys. This study was supported by the research projects: PGC2018-100914-B-100, UPO-1259543, "Monitorizacion hidrológica y modelización de la relación laguna-acuífero en los mantos eólicos de Doñana" of the Ministerio de Economía y Competitividad of Spain, Fondo Europeo de Desarrollo Regional FEDER and Guadalquivir River Basin Authority and "Tectonic conditioning and climate change effects on the hydrogeological evolution of wetlands and playa-lakes in the southern Spain" from the University of Pablo de Olavide.

References

Aguirre, J., Braga, J. C., Martín-Pérez, J. A., Martín, J. M. and Puga-Bernabéu, Á., 2022. Upper Miocene deposits at the southern margin of the Guadalquivir Foreland Basin (central Betic Cordillera, S. Spain). Implications for the closure timing of the Atlantic-Mediterranean connections. *Revue de Micropaléontologie*, *76*, 100690. https://doi.org/10.1016/j.revmic.2022.100690

Andreo, B., Gil-Márquez, J. M., Mudarra, M., Linares, L. and Carrasco, F., 2016. Hypothesis on the hydrogeological context of wetland areas and springs related to evaporitic karst aquifers

(Málaga, Córdoba and Jaén provinces, Southern Spain). *Environmental Earth Sciences*, *75*, 1-19. https://doi.org/10.1007/s12665-016-5545-1

Antón L., De Vicente G., Muñoz-Martin A., Stokes M. (2014). Using river profiles and geomorphic indices to evaluate geomorphological signature of continental scale drainage capture, Duero basin (NW Spain). Geomorphology, 206, 250-261, https://doi.org/10.1016/j.geomorph.2013.09.028

Babault, J., Van Den Driessche, J. and Teixell, A., 2012. Longitudinal to transverse drainage network evolution in the High Atlas (Morocco): The role of tectonics. *Tectonics*, *31*(4). https://doi.org/10.1029/2011TC003015

Balanyá, J. C., Crespo-Blanc, A., Díaz Azpiroz, M., Expósito, I. and Luján, M., 2007. Structural trend line pattern and strain partitioning around the Gibraltar Arc accretionary wedge: insights as to the mode of orogenic arc building. *Tectonics*, *26*(2). https://doi.org/10.1029/2005TC001932

Balanya, J. C., Crespo-Blanc, A., Díaz-Azpiroz, M., Expósito, I., Torcal, F., Pérez-Peña, V. and Booth-Rea, G. (2012). Arc-parallel vs back-arc extension in the Western Gibraltar arc: Is the Gibraltar forearc still active?. *Geologica Acta: an international earth science journal*, *10*(3), 249-263.

Barcos, L., Balanyá, J. C., Díaz-Azpiroz, M., Expósito, I., & Jiménez-Bonilla, A. (2015). Kinematics of the Torcal Shear Zone: Transpressional tectonics in a salient-recess transition at the northern Gibraltar Arc. *Tectonophysics*, *663*, 62-77. https://doi.org/10.1016/j.tecto.2015.05.002

Barcos, L., Díaz-Azpiroz, M., Balanyá, J. C., Expósito, I., Jiménez-Bonilla, A. and Faccenna, C., 2016. Analogue modelling of inclined, brittle–ductile transpression: testing analytical models through natural shear zones (external Betics). *Tectonophysics*, *682*, 169-185. https://doi.org/10.1016/j.tecto.2016.05.021

Berry M., Wijk J. van, Emry E., García-Castellanos D. (2019). Endorheic-Exorheic transitions of the Río Grande and East African Rifts. Geochemistry, Geophysics and Geosystems, 20, 3705-3729, https://doi.org/10.1029/2018GC008176

https://doi.org/10.5194/egusphere-2025-538
Preprint. Discussion started: 25 February 2025

Blanc, P. L., 2006. Improved modelling of the Messinian Salinity Crisis and conceptual implications. *Palaeogeography, Palaeoclimatology, Palaeoecology*, *238*(1-4), 349-372. https://doi.org/10.1016/j.palaeo.2006.03.033

Braga, J. C., Martín, J. M. and Quesada, C., 2003. Patterns and average rates of late Neogene–Recent uplift of the Betic Cordillera, SE Spain. *Geomorphology*, *50*(1-3), 3-26. https://doi.org/10.1016/S0169-555X(02)00205-2

Calaforra, J. M. and Pulido-Bosch, A., 1999. Gypsum karst features as evidence of diapiric processes in the Betic Cordillera, Southern Spain. *Geomorphology*, *29*(3-4), 251-264. https://doi.org/10.1016/S0169-555X(99)00019-7

Comino, J., and Senciales, J.M., 2012.Las plataformas travertínicas y tobáceas de la provincia de Málaga (España). Baetica. Estudios de Arte, Geografía e Historia, 34, 2012, 83-102.

Davis, D., Suppe, J. and Dahlen, F. A., 1983. Mechanics of fold-and-thrust belts and accretionary wedges. *Journal of Geophysical Research: Solid Earth*, *88*(B2), 1153-1172. https://doi.org/10.1029/JB088iB02p01153

Díaz-Azpiroz, M., Barcos, L., Balanyá, J. C., Fernández, C., Expósito, I. and Czeck, D. M., 2014. Applying a general triclinic transpression model to highly partitioned brittle-ductile shear zones: A case study from the Torcal de Antequera massif, external Betics, southern Spain. *Journal of Structural Geology*, *68*, 316-336. https://doi.org/10.1016/j.jsg.2014.05.010

Díaz Azpiroz, M., Asencio Almansa, R., Senín Andrades, J. R., & Jiménez Bonilla, A. 2020. Shape preferred orientation of dolostone bodies of a Triassic broken formation at the western External Betics.

Díaz-Azpiroz, M., Jiménez-Bonilla, A., Frontera, T., Expósito, I. and Balanyá, J.C., (2022). Strain partitioning at the active mountain front of the western Betics (southern Spain). European Society for Deformation Mechanisms, Rheology and Tectonics. DRT 2022. Catania.

https://doi.org/10.5194/egusphere-2025-538
Preprint. Discussion started: 25 February 2025

Elez, J., Silva, P. G., Huerta, P., Perucha, M. Á., Civis, J., Roquero, E. and Martínez-Graña, A., 2016. Quantitative paleotopography and paleogeography around the Gibraltar arc (South Spain) during the Messinian salinity crisis. *Geomorphology*, *275*, 26-45. https://doi.org/10.1016/j.geomorph.2016.09.023

Elez, J., Silva, P. G., Huerta, P. and Martínez-Graña, A., 2018. Isostatic compensation in the Western-Central Betic Cordillera (South Spain) caused by erosional unloading from the Messinian to the present: the emergence of an orogen. *Geogaceta*, *64*, 103-106.

Elez, J., Silva, P. G. and Martínez-Graña, A. M., 2020. Quantification of Erosion and Uplift in a Rising Orogen—A Large-Scale Perspective (Late Tortonian to Present): The Case of the Gibraltar Arc, Betic Cordillera, Southern Spain. *Remote Sensing*, *12*(21), 3492.

England, P. and Molnar, P., 1990. Surface uplift, uplift of rocks, and exhumation of rocks. *Geology*, *18*(12), 1173-1177. https://doi.org/10.1130/0091-7613(1990)018<1173:SUUORA>2.3.CO;2

Ercilla, G., Juan, C., Periáñez, R., Alonso, B., Abril, J. M., Estrada, F. and Valencia, J., 2019. Influence of alongslope processes on modern turbidite systems and canyons in the Alboran Sea (southwestern Mediterranean). *Deep Sea Research Part I: Oceanographic Research Papers*, *144*, 1-16. https://doi.org/10.1016/j.dsr.2018.12.002

Expósito, I., Jiménez-Bonilla, A., Delchiaro, M., Yanes, J. L., Balanyá, J. C., Moral-Martos, F. and Della Seta, M., 2022. Geomorphic signature of segmented relief rejuvenation in the Sierra Morena, Betic forebulge, Spain. *Earth Surface Dynamics*, *10*(5), 1017-1039. https://doi.org/10.5194/esurf-10-1017-2022

Expósito, I., Balanyá, J. C., Crespo-Blanc, A., Díaz-Azpiroz, M. and Luján, M., 2012. Overthrust shear folding and contrasting deformation styles in a multiple decollement setting, Gibraltar Arc external wedge. *Tectonophysics*, *576*, 86-98. https://doi.org/10.1016/j.tecto.2012.04.018

Farines, B., Calvet, M., & Gunnell, Y. (2015). The summit erosion surfaces of the inner Betic Cordillera: Their value as tools for reconstructing the chronology of topographic growth in southern Spain. Geomorphology, 233, 92-111. https://doi.org/10.1016/j.geomorph.2014.11.019

Fernandez, C., Czeck, D. M., & Diaz-Azpiroz, M. (2013). Testing the model of oblique transpression with oblique extrusion in two natural cases: steps and consequences. *Journal of Structural Geology*, *54*, 85-102. https://doi.org/10.1016/j.jsg.2013.07.001

Fuentes, P., Fernández, C., Díaz-Alvarado, J. and Díaz-Azpiroz, M., 2019. Using 3D kinematic models in subduction channels. The case of the Chañaral tectonic mélange, Coastal Cordillera, northern Chile. *Gondwana Research*, *74*, 251-270. https://doi.org/10.1016/j.gr.2018.12.009

Garcia-Alix, A., Jimenez-Moreno, G., Gazquez, F., Monedero-Contreras, R., López-Avilés, A., Jimenez-Espejo, F. J., ... & Anderson, R. S. (2022). Climatic control on the Holocene hydrology of a playa-lake system in the western Mediterranean. Catena, 214, 106292. https://doi.org/10.1016/j.catena.2022.106292

Giano S.I. and Schiattarella M. (2023). Drainage integration of small endorheic basins at the Pleistocene-Holocene transition: An example from southern Italy. Geomorphology, 427, https://doi.org/10.1016/j.geomorph.2023.108622

Gil-Márquez, J. M., Barberá, J. A., Andreo, B. and Mudarra, M., 2017. Hydrological and geochemical processes constraining groundwater salinity in wetland areas related to evaporitic (karst) systems. A case study from Southern Spain. *Journal of Hydrology*, *544*, 538-554. https://doi.org/10.1016/j.jhydrol.2016.11.062

Giletycz, S., Loget, N., Chang, C. P. and Mouthereau, F., 2015. Transient fluvial landscape and preservation of low-relief terrains in an emerging orogen: example from Hengchun Peninsula, Taiwan. *Geomorphology*, *231*, 169-181. https://doi.org/10.1016/j.geomorph.2014.11.026

Harkins, N., Kirby, E., Heimsath, A., Robinson, R. and Reiser, U., 2007. Transient fluvial incision in the headwaters of the Yellow River, northeastern Tibet, China. *Journal of Geophysical Research: Earth Surface*, *112*(F3). **https://doi.org/10.1029/2006JF000570**

Höbig, N., Mediavilla, R., Gibert, L., Santisteban, J. I., Cendón, D. I., Ibáñez, J. and Reicherter, K., 2016. Palaeohydrological evolution and implications for palaeoclimate since the Late Glacial at Laguna de Fuente de Piedra, southern Spain. *Quaternary International*, *407*, 29-46. https://doi.org/10.1016/j.quaint.2016.02.051

Jiménez Bonilla, A., Barcos, L., Expósito, I., Balanyá, J. C. and Díaz Azpiroz, M., 2013. La Zona Transversal de Peñarrubia-Almargen (Béticas): tectónica transpresiva tardía y segmentación del relieve. Geogaceta 55, 7-10.

Jiménez-Bonilla, A., Expósito, I., Balanyá, J. C., Díaz-Azpiroz, M. and Barcos, L., 2015. The role of strain partitioning on intermontane basin inception and isolation, External Western Gibraltar Arc. *Journal of Geodynamics*, *92*, 1-17. https://doi.org/10.1016/j.jog.2015.09.001

Jiménez-Bonilla, A., Expósito, I., Balanyá, J. C., & Díaz-Azpiroz, M., 2017. Strain partitioning and relief segmentation in arcuate fold-and-thrust belts: a case study from the western Betics. *Journal of Iberian Geology*, *43*, 497-518. https://doi.org/10.1007/s41513-017-0028-0

Jiménez-Bonilla, A., Díaz-Azpiroz, M., Rodríguez, M. R. (2023). Tectonics may affect closed watersheds used to monitor climate change and human activity effects. *Terra Nova*, *35*(1), 58-65. **https://doi.org/10.1111/ter.12629**

Jiménez-Bonilla, A., Crespo-Blanc, A., Balanyá, J. C., Expósito, I. and Díaz-Azpiroz, M., 2020. Analog models of fold-and-thrust wedges in progressive arcs: a comparison with the Gibraltar Arc external wedge. *Frontiers in Earth Science*, *8*, 72.

Junta de Andalucía, 2016. (http://www. juntadeandalucia.es/institutodeestadisticaycartografia/prod Cartografia/bc/mdt.htm)

Keller, G. R., 1986. Introduction to special section on the Rio Grande rift. *Journal of Geophysical Research: Solid Earth*, *91*(B6), 6142-6142.

Keller, E. A. and Pinter, N., 1996. *Active tectonics* (Vol. 338). Upper Saddle River, NJ: Prentice Hall.

Korup, O., 2006. Rock-slope failure and the river long profile. *Geology*, *34*(1), 45-48. https://doi.org/10.1130/G21959.1

Lhénaff, R. (1967). *Recherches Geomorphologiques sur les cor Dilleres Betiques Centre accidentales* (Doctoral dissertation, PhD. thesis, Univ. de Lille 1, Villeneuve d'Ascq, France).

https://doi.org/10.5194/egusphere-2025-538
Preprint. Discussion started: 25 February 2025

Loget, N. and Van Den Driessche, J., 2006. On the origin of the Strait of Gibraltar. *Sedimentary Geology*, *188*, 341-356. https://doi.org/10.1016/j.sedgeo.2006.03.012

Luján, M., Crespo-Blanc, A. and Comas, M., 2011. Morphology and structure of the Camarinal Sill from high-resolution bathymetry: evidence of fault zones in the Gibraltar Strait. *Geo-Marine Letters*, *31*, 163-174. https://doi.org/10.1007/s00367-010-0222-y

Madof, A. S., Bertoni, C. and Lofi, J., 2019. Discovery of vast fluvial deposits provides evidence for drawdown during the late Miocene Messinian salinity crisis. *Geology*, *47*(2), 171-174. https://doi.org/10.1130/G45873.1

Martin, J. M., Braga, J. C. and Betzler, C., 2001. The Messinian Guadalhorce corridor: the last northern, Atlantic–Mediterranean gateway. *Terra Nova*, *13*(6), 418-424.

https://doi.org/10.1046/j.1365-3121.2001.00376.x

Martín, J. M., Braga, J. C., Aguirre, J. and Puga-Bernabéu, Á., 2009. History and evolution of the North-Betic Strait (Prebetic Zone, Betic Cordillera): a narrow, early Tortonian, tidal-dominated, Atlantic–Mediterranean marine passage. *Sedimentary Geology*, *216*(3-4), 80-90. https://doi.org/10.1016/j.sedgeo.2009.01.005

Martín Martín, J. M., Puga Bernabeu, Á., Aguirre Rodríguez, J. and Braga Alarcón, J. C., 2014. Miocene Atlantic-Mediterranean seaways in the Betic Cordillera (Southern Spain).

Mather A.E. (2000). Adjustement of a drainage network to capture induced base-level change: an example from the Sorbas Basin, S. Spain. Geomorphology, 34, 271-289. https://doi.org/10.1016/S0169-555X(00)00013-1

Medialdea, T., Suriñach, E., Vegas, R., Banda, E. and Ansorge, J., 1986. Crustal structure under the western end of the Betic Cordillera (Spain). In *Annales geophysicae. Series B. Terrestrial and planetary physics* (Vol. 4, No. 4, pp. 457-464).

Medina, F. C. (1991). Mapa Geológico de España E. 1: 50.000.

https://doi.org/10.5194/egusphere-2025-538
Preprint. Discussion started: 25 February 2025

Pérez-Peña, J. V., Azañón, J. M., Azor, A., Delgado, J., & González-Lodeiro, F. (2009). Spatial analysis of stream power using GIS: SLk anomaly maps. *Earth Surface Processes and Landforms*, *34*(1), 16-25. **https://doi.org/10.1002/esp.1684**

Pérez-Peña, J. V., Azor, A., Azañón, J. M. and Keller, E. A. (2010). Active tectonics in the Sierra Nevada (Betic Cordillera, SE Spain): Insights from geomorphic indexes and drainage pattern analysis. *Geomorphology*, *119*(1-2), 74-87. https://doi.org/10.1016/j.geomorph.2010.02.020

Perron, J. T. and Royden, L., 2013. An integral approach to bedrock river profile analysis. *Earth surface processes and landforms*, *38*(6), 570-576.

https://doi.org/10.1002/esp.3302

Recio-Ruiz, A. and Ruíz-Somovilla, I., 1990. Prospecciones arqueológicas en el T.M. de Sierra de Yeguas (Málaga). Prospecciones arqueológicas, 11- 12, 93–110.

Repasch M., Karlstrom K.E., Heizler M., Pecha M. (2017). Birth and evolution of the Rio Grande fluvial system in the past 8 Ma: Progressive downward integration and the influence of tectonics, volcanism, and climate. Earth-Science Reviews, 168, 113-164. https://doi.org/10.1016/j.earscierev.2017.03.003

Rodríguez-Rodríguez, M., 2007. Hydrogeology of ponds, pools, and playa-lakes of southern Spain. *Wetlands*, *27*(4), 819-830.

Rodríguez-Rodríguez, M., Moral, F. and Benavente, J. 2009. Grado de dependencia de las aguas subterráneas, índice de funcionamiento hidrológico y principales amenazas en los principales humedales continentales de la depresión del Guadalquivir. *Boletín Geológico y Minero*, *120*(3), 347-360.

Rodríguez-Rodríguez, M., Moral, F., Benavente, J. and Beltrán, M., 2010. Developing hydrological indices in semi-arid playa-lakes by analyzing their main morphometric, climatic and hydrochemical characteristics. *Journal of Arid Environments*, *74*(11), 1478-1486. https://doi.org/10.1016/j.jaridenv.2010.03.018

Rodríguez-Rodríguez, M., Green, A. J., López, R. and Martos-Rosillo, S., 2012. Changes in water level, land use, and hydrological budget in a semi-permanent playa lake, Southwest Spain.

https://doi.org/10.5194/egusphere-2025-538
Preprint. Discussion started: 25 February 2025

Environmental Monitoring and Assessment, *184*, 797-810. https://doi.org/10.1007/s10661-011-2002-1

Rodriguez-Rodriguez, M., Martos-Rosillo, S. and Pedrera, A., 2016. Hydrogeological behaviour of the Fuente-de-Piedra playa lake and tectonic origin of its basin (Malaga, southern Spain). *Journal of Hydrology*, *543*, 462-476. https://doi.org/10.1016/j.jhydrol.2016.10.021

Roveri, M., Flecker, R., Krijgsman, W., Lofi, J., Lugli, S., Manzi, V. and Stoica, M., 2014. The Messinian Salinity Crisis: past and future of a great challenge for marine sciences. *Marine Geology*, *352*, 25-58. https://doi.org/10.1016/j.margeo.2014.02.002

Ruiz-Constán, A., Pedrera, A., Galindo-Zaldívar, J., Pous, J., Arzate, J., Roldán-García, F. J. and Anahnah, F., 2012. Constraints on the frontal crustal structure of a continental collision from an integrated geophysical research: The central-western Betic Cordillera (SW Spain). *Geochemistry, Geophysics, Geosystems*, *13*(8). **https://doi.org/10.1029/2012GC004153**

Sanderson, D. J., & Marchini, W. R. D. (1984). Transpression. *Journal of structural Geology*, *6*(5), 449-458. https://doi.org/10.1016/0191-8141(84)90058-0

Sanz de Galdeano, C. and Alfaro, P., 2004. Tectonic significance of the present relief of the Betic Cordillera. *Geomorphology*, *63*(3-4), 175-190. https://doi.org/10.1016/j.geomorph.2004.04.002

Schoorl, J. M. and Veldkamp, A., 2003. Late Cenozoic landscape development and its tectonic implications for the Guadalhorce valley near Alora (Southern Spain). *Geomorphology*, *50*(1-3), 43-57. https://doi.org/10.1016/S0169-555X(02)00207-6

Schulmann, K., Thompson, A. B., Lexa, O. and Ježek, J., 2003. Strain distribution and fabric development modeled in active and ancient transpressive zones. *Journal of Geophysical Research: Solid Earth*, *108*(B1), ETG-6. **https://doi.org/10.1029/2001JB000632**

Sobel E.R., Hilley G.E., Strecker M.R. (2003). Formation of internally drained contractional basins by aridity-limited bedrock incision. Journal of Geophysical Research, 108, https://doi.org/10.1029/2002JB001883

https://doi.org/10.5194/egusphere-2025-538
Preprint. Discussion started: 25 February 2025

931 Stokes M., Mather A.E., Kearsey S.H., Lewin S. (2019). Anatomy, Age and Origin of an
932 Intramontane Top Basin Surface (Sorbas Basin, Betic Cordillera, S. Spain). Quaternary, 1, 15,
933 https://doi.org/10.3390/quat1020015

934 Torné, M. and Banda, E., 1992. Crustal thinning from the Betic Cordillera to the Alboran Sea.
935 *Geo-Marine Letters*, *12*, 76-81. https://doi.org/10.1007/BF02084915

936 Vera, J. A., 2004. Geología de España. Instituto Geológico y Minero de España (IGME), Madrid,
937 884 p. *Geology of Spain"*.

938 Whipple, K. X. and Tucker, G. E., 1999. Dynamics of the stream-power river incision model:
939 Implications for height limits of mountain ranges, landscape response timescales, and research
940 needs. *Journal of Geophysical Research: Solid Earth*, *104*(B8), 17661-17674.

941 **https://doi.org/10.1029/1999JB900120**

942 Willett, S. D., McCoy, S. W., Perron, J. T., Goren, L. and Chen, C. Y., 2014. Dynamic
943 reorganization of river basins. *Science*, *343*(6175), 1248765. DOI: 10.1126/science.1248765

944 Winterberg, S. and Willett, S. D., 2019. Greater Alpine river network evolution, interpretations
945 based on novel drainage analysis. *Swiss Journal of Geosciences*, *112*, 3-22.
946 https://doi.org/10.1007/s00015-018-0332-5